Cell. Mol. Life Sci. 64 (2007) 230–243
1420-682X/07/020230-14
DOI 10.1007/s00018-006-6412-0

Cellular and Molecular Life Sciences

Research Article

Autotaxin (NPP-2) in the brain: cell type-specific expression and regulation during development and after neurotrauma

N. E. Savaskan [a, *], L. Rocha [b], M. R. Kotter [c], A. Baer [c], G. Lubec [c], L. A. van Meeteren [a], Y. Kishi [d], J. Aoki [d], W. H. Moolenaar [a], R. Nitsch [b] and A. U. Bräuer [b, *]

[a] Division of Cellular Biochemistry, The Netherlands Cancer Institute, Amsterdam (The Netherlands), e-mail: n.savaskan@nki.nl
[b] Institute for Cell Biology and Neurobiology, Center for Anatomy, Charité – Universitätsmedizin Berlin, 10115 Berlin (Germany), Fax: +49 30 450 528 908, e-mail: anja.braeuer@charite.de
[c] Department of Neurosurgery, BrainProt Neuroprotection-Neuroregeneration Laboratory, AKH/Medical University Vienna, Vienna (Austria)
[d] Graduate School of Pharmaceutical Sciences, The University of Tokyo, Tokyo (Japan), PRESTO, Japan Science and Technology Agency

Received 18 September 2006; received after revision 30 October 2006; accepted 4 December 2006
Online First 27 December 2006

Abstract. Autotaxin is a secreted cell motility-stimulating exo-phosphodiesterase with lysophospholipase D activity that generates bioactive lysophosphatidic acid. Lysophosphatidic acid has been implicated in various neural cell functions such as neurite remodeling, demyelination, survival and inhibition of axon growth. Here, we report on the *in vivo* expression of autotaxin in the brain during development and following neurotrauma. We found that autotaxin is expressed in the proliferating subventricular and choroid plexus epithelium during embryonic development. After birth, autotaxin is mainly found in white matter areas in the central nervous system. In the adult brain, autotaxin is solely expressed in leptomeningeal cells and oligodendrocyte precursor cells. Following neurotrauma, autotaxin is strongly up-regulated in reactive astrocytes adjacent to the lesion. The present study revealed the cellular distribution of autotaxin in the developing and lesioned brain and implies a function of autotaxin in oligodendrocyte precursor cells and brain injuries.

Keywords. LPA signaling, S1P, axonal growth and regeneration, hippocampus, brain development, G protein-coupled receptors, myelination, oligodendrocyte precursor cells.

Introduction

Lysophosphatidic acid (LPA) is a major bioactive lipid in serum, involved in fundamental cellular functions, including cell proliferation and differentiation, migration, adhesion, cell survival and morphogenesis [1–4]. LPA mediates its multiple cellular effects through G protein-coupled receptors (LPA_{1-5}/EDG_{1-3}), with subsequent activation of phospholipase C and D (PLC and PLD), Ca^{2+} liberation, and activation of monomeric GTPases [5–7] and can be detected in various biological fluids, such as serum, saliva, seminal fluid, and follicular and cerebrospinal fluids [8–13]. Additionally, LPA levels are elevated under diverse pathophysiological conditions, such as ovarian cancer, atherosclerotic lesion, and in the nervous system following damage [14–16]. In the developing brain, LPA has been implicated in the regulation of cortical neurogenesis and pattern formation [4]. Until the recent discovery of autotaxin (ATX), it was unclear by which mechanism and through which enzymes bioactive LPA is produced. Purification studies, however, have revealed that the soluble ATX enzyme (also named nucleotide pyrophosphatase-phosphodiesterase 2/NPP-2, lysoPLD or PD-Iα) is responsible for generating extra-

* Corresponding author.

cellular LPA [17, 18]. Although it has been shown that postmitotic neurons can potentially produce LPA or an LPA-like activity in the brain, and thereby modulate cortical pattern formation [5], the exact cellular distribution and expression kinetics of ATX during brain development and its possible regulation following neurotrauma remain largely unknown.

ATX is an extracellular enzyme of 125 kDa, which was originally identified as an autocrine tumor cell motility-stimulating factor overexpressed in a variety of human cancers including primary brain tumors [10, 14, 19–23]. It belongs to the nucleotide pyrophosphatase and phosphodiesterase (NPP) family, which to date comprises seven enzymes [24–29]. However, despite their structurally related catalytic domain, ATX is unique in its receptor-active LPA-generating activity, whereas the other six NPP family members (NPP1, NPP3-NPP7) lack intrinsic lysoPLD activity [26–28, 30, 31]. Initially, ATX was considered a type II transmembrane protein that contains a very short N-terminal cytosolic domain, a single transmembrane domain, two cysteine-rich somatomedin B-like domains, and a large catalytic ectodomain [3, 25]. However, three independent studies have recently shown that ATX is synthesized as a pre-pro-enzyme and is secreted by the classical secretory pathway by intracellular cleavage of an N-terminal 27 residue signal peptide sequence [21, 31, 32].

The vital role of ATX in development has recently been established since ATX deletion in mice is lethal at embryonic day 9.5–10.5 [33, 34]. ATX-null mutants do not develop mature vessels and show massive neural tube defects and asymmetric headfolds, indicating a critical role for ATX in vascular and neuronal development [33, 34]. ATX transcription was first detected in the floor plate of the neural tube [35] by means of *in situ* hybridization techniques. Further studies on postnatal day 7 to 10 (P7–10) rodents revealed ATX mRNA in the ventral horn of the spinal cord, optic nerve, choroid plexus, and in the cerebellum [36, 37]. A separate study also found ATX in the retina [38]. Within the postnatal optic nerve, ATX was predominantly associated with myelin oligodendorcyte glycoprotein (MOG)- and proteolipid protein (PLP/DM20)-positive oligodendrocytes and the choroid plexus epithelium [36–39]. However, despite the fact that secreted ATX can generate LPA and sphingosine-1-phosphate (S1P) from preexisting lysophosphaditylcholine and other lysophospholipids [18, 40, 41], its exact cellular and subcellular distribution and developmental, as well as post-trauma, regulation in the brain remain unknown.

Here, we report on *in vivo* ATX gene and protein expression in the developing and adult brain, with particular emphasis on the cortex and hippocampus. We show that ATX is mainly found in white matter regions, the choroid plexus, leptomeninges and in the subventricular zone. To gain further insight into the possible functional role of ATX in the brain, we analyzed its cellular expression in the brain under physiological conditions and following trauma. We unambiguously demonstrate that, under physiological conditions, ATX is restricted to early oligodendrocyte lineage cells (OLCs), choroid plexus epithelial and leptomeningeal cells, whereas neurons and astrocytes are negative for ATX expression. Within these cells, ATX appears to be in vesicles and vesicle-like structures, supporting previous results identifying ATX as a secreted enzyme, rather than a type II transmembrane protein [21, 32]. However, following brain lesion, reactive astrocytes adjacent to the lesion site appear to express ATX. Thus, these data reveal the cellular distribution of ATX in the developing and lesioned brain, and suggest a role for ATX in early OLCs as well as in neural reorganization after acute phases of injury to the central nervous system (CNS).

Material and methods

Animals, neurotrauma induction, and tissue isolation. Pregnant and adult male Sprague rats (200 g–250 g weight) obtained from our central animal facility (Tierexperimentelle Einrichtung Charité) were kept under standard laboratory conditions, conforming to German and European guidelines for the use of laboratory animals (in accordance with 86/609/EEC). The birth of each litter was recorded and determined as P0. All surgical procedures were performed in adherence to European and German law on the use of laboratory animals. For stereotactic surgery, the rats were anesthetized with a mixture of 25 mg/ml Ketamin (CuraMed Pharma GmbH, Germany), 1.2 mg/ml Xylazin (Bayer, Germany) and 0.35 mg/ml Acepromazin (Sanofi GmbH, Germany) in 0.9% sterile NaCl (2.5 ml/kg body weight i.p.) and received a unilateral entorhinal cortex lesion (ECL) using a stereotaxic headholder (Stoelting, Germany). In brief, a standard electrocoagulator was used to make bilateral incisions [with four single pulses (2.5 μA) for 3 s each] in the frontal and sagittal planes between the entorhinal cortex and hippocampus. The following coordinates were used, measuring from the lambda: frontal incision: AP +1.2, L 3.1 to 6.1, and V down to the inferior cranium; sagittal incision: AP +1.2 to +4.2, L 6.1, and V down to the inferior cranium [42]. The rats were allowed to survive for 1, 10, and 21 days (n=4 animals per stage) for *in situ* hybridization, and 2, 5, and 12 days (n=3 animals per stage) for immunocytochemistry, and were then decapitated under deep ether anesthesia (Chinosol, Germany). Their brains and spinal cord were immediately frozen in liquid nitrogen and stored at –80 °C.

***In situ* hybridization.** For the *in situ* hybridization experiments, four brains per time point were dissected and fro-

zen in the gaseous phase of liquid nitrogen. For improved hybridization and resolution quality and for technical reasons, two of three meninges, the dura mater and arachnoid mater, were removed, whereas the pia mater was left. Horizontal cryostat sections (15 µm) were fixed in 4% paraformaldehyde (w/v), washed in 0.1 M phosphate-buffered saline (PBS, pH 7.4) and dehydrated. For *in situ* hybridization, the following oligonucleotides were used: antisense oligonucleotides (5′-ATATTACCTGGAATGACCCGAGACAGCCTTGTCTTGCCATG-3′) and (5′-CACGTAGGCCATCGTAATTGTAGTCAAAAATCGGTCCAC-3′), which are complementary to rat ATX mRNA (GenBank accession number NM_057104) and its sense oligonucleotides. While both oligonucleotides were investigated and led to essentially the same results, only the latter is discussed in the present study. The specificity of the oligonucleotides was confirmed by BLAST GenBank search (www.ncbi.nlm.nih.gov) and showed no significant crossmatches with known sequences and ESTs. The oligonucleotides were end-labeled using terminal desoxynucleotide transferase (Boehringer, Germany) and [α-^{35}S]dATP (DuPont NEN, USA), and used for *in situ* hybridization. Hybridization was performed for 16 h at 42 °C in a humidified chamber, after which the slides were washed as follows: 2 × 30 min in 1× SSC at 56 °C and 1 × 10 min in 0.5× SSC at room temperature. Finally, the sections were rinsed in H_2O at room temperature and dehydrated. The slides were then exposed to Kodak X-OMAT AR X-ray film for autoradiography for 20 days. Sections hybridized with labeled sense oligonucleotides and sections hybridized with antisense oligonucleotides in the presence of unlabeled (cold) antisense oligonucleotides in 40-fold surplus served as controls. These controls showed only background hybridization signals. After exposure, the slides were counterstained with toluidine blue [43].

RNA isolation, quantitative RT-PCR and ATX transcriptional analysis. Total RNA from whole rat brain lysate at various developmental stages was isolated using the ISOGEN kit (Nippongene, Japan). Messenger RNA from different cell lines, including HEK293 and COS-7 cells, was isolated with the Qiagen mRNA kit (Germany). Reverse transcription was performed, using the SuperScript First-Strand Synthesis System from Invitrogen (USA). Oligonucleotide primers for qRT-PCR were designed with Primer Express software (Applied Biosystems, USA). For rat LPA_1 and ATX cDNA detection, the following primers were used: LPA_1 forward – GAATCGGACACCATGAT; LPA_1 reverse – ATCCCGGAGTCCAGCAG; ATX forward – AATCGGGATACCATGATGAGTCTT; ATX reverse – CCAGGAGTCCAGCAGATGATAAA; an alternative primer set was used for cell culture PCR: ATX forward primer: – GGATTATGTACCTTCAGTC; ATX reverse primer: – GTGATGATGCTGTAGTAGTG. Normalization was performed with GAPDH as an internal standard to ensure RNA integrity and an equal amount of input cDNA: GAPDH forward – GCCAAGGTCATCCATGACAACT; GAPDH reverse – GAGGGGCCATCCACAGTCTT. PCR reactions were analyzed using an ABI Prism 7000 Sequence detection system (Applied Biosystems, USA). The number of transcripts was quantified and each sample normalized on the basis of GAPDH content.

Antibody generation, specificity testing and immunoblotting. Generation of ATX-specific monoclonal antibodies (mAbs) was performed by expressing a polypeptide (amino acid numbers 58–182 of the human ATX sequence) in *E. coli* as a GST-fusion protein using the pGEX-4T vector (Amersham Bioscience, UK) as described by Baumforth et al. [22]. Briefly, the protein was purified using GSH-Sepharose according to the manufacturer's recommended protocol. The GST fusion protein was used to immunize rats (WKY/Izm strain) by injection into the hind footpads with Freund's complete adjuvant. The enlarged medial iliac lymph nodes from these rats were used for cell fusion with mouse myeloma cells (PAI). The antibody-secreting hybridoma cells were selected by screening with an enzyme-linked immunosorbent assay, as well as immunofluorescence and immunoblotting techniques. We established three antibody-secreting hybridoma cell lines. The mAb clone 4F1 was found to react with human, mouse, rat, and bovine ATX in immunoblotting analysis and was used in this study. For antibody specificity and comparison analysis, we transfected COS-7 cells (which do not endogenously express ATX) with a human ATX-pcDNA-GFP plasmid, using an electroporation approach (Amaxa Biosystems, Germany). In addition, we used a commercially available anti-ATX antibody (Cayman, MI, USA), which produced essentially the same immunostaining and immunoblot results as the former ATX preparation. At 48 h after transfection, cells were harvested and lysed in ice-cold total lysis buffer as previously described [44]. Cleared total cell lysates were separated by 10% SDS-PAGE and transferred to nitrocellulose membranes. The membranes were probed with anti-ATX mAb or anti-green fluorescent protein (GFP; Invitrogen, Germany). The immunocomplexes were detected by enhanced chemiluminescence (Amersham, UK). For Western blot analysis, total protein extracts from adult rat control hippocampus tissue at 2 and 5 days after lesion were separated on a 12% SDS-PAGE and electroblotted onto a nitrocellulose membrane. Membranes were blocked overnight with 10% non-fat milk/PBS and probed with anti-ATX mAb (clone 4F1) for 48 h at 4 °C. Immunoreactive bands were identified with horseradish peroxidase-conjugated anti-rat secondary antibodies, followed by chemiluminescence (Amersham, UK). β-Actin expression was used as an internal control for standardization of the protein amount. Western blot quantification was performed with

a computerized videodensitometry system (Metamorph, Universal Imaging, USA). Analysis was performed using the Mann-Whitney U-test (Statview II, USA). The level of significance was set at $p < 0.05$.

Immunocytochemistry. Animals were deeply anesthetized with a Ketamin mixture as described previously and perfused by vascular injection with 0.9% NaCl solution, followed by 4% paraformaldehyde in 0.1 M sodium phosphate buffer, pH 7.4 [43]. Brains were removed and cut on a vibratome. The immunocytochemistry procedure and buffers have been described in detail previously [43]. Briefly, in horizontal brain sections (40 µm), the endogenous peroxidase was quenched in 0.5% hydrogen peroxide diluted in PBS. After washing, the brain sections were quenched again in 50 mM NH_4Cl/PBS for 30 min. The sections were blocked with 10% goat serum/0.1% saponin in PBS for 1 h at room temperature and exposed to anti-ATX mAb (diluted 1 : 200 in blocking solution) at 4 °C for 48 h. After washing in PBS/0.1% saponin, the sections were incubated with anti-rat biotinylated antisera overnight at 4 °C and then in avidin-biotin peroxidase complex reagent (Vectastain ABC Kit, USA) for 2 h at room temperature. The immunoreaction was visualized with 3,3′-diaminobenzidine as a chromogen.

Double-labeling immunofluorescence. For simultaneous detection of the ATX antigen with specific cell types, additional double-labeling immunofluorescence experiments were performed using the glial marker glial fibrillary acidic protein (GFAP) for astrocytes, IB4 for microglia, cyclic 2′3′nucleotide phosphodiesterase (CNPase) for oligodendrocytes, and the neuronal marker MAP-2. For stage-specific characterization of oligodendrocytes, the following markers were used: NG2 and A2B5 for early oligodendrocyte precursors, O4 for late oligodendrocytes and CC1 for mature oligodendrocytes. First, the paraformaldehyde-fixed sections were processed for ATX detection as described above. Next, the anti-ATX antibody was detected with Alexa-488-labeled goat anti-rat antibody (Molecular Probes, USA, diluted 1 : 500). In addition to the first incubation, the sections or cells were incubated overnight with anti-GFAP (DAKO, Denmark), anti-IB4 (Sigma, USA), anti-CNPase mAb (Sigma, USA), anti-CC1 mAb (Calbiochem, USA), anti-NG2 mAb (Chemicon, USA), anti-A2B5 mAb (Chemicon, USA), anti-O4 mAb (Chemicon, USA), or anti-MAP-2 mAb (Sigma, USA). The second antibodies for co-localization were detected with an Alexa-594-labeled antibody (Molecular Probes, USA) and sections were mounted with Immu-Mount (Shandon, USA). The sections and cultured cells were imaged using an upright Leica confocal microscope (TCS) or on a Leica DM LB microscope equipped with a CCD camera.

Cell culture. COS-7 cells (ATCC: CRL-1651) and HEK 293 cells were routinely maintained at 37 °C with 5% CO_2 in Dulbecco's modified Eagle's medium supplemented with 10% fetal bovine serum, 100 U/ml penicillin, and 100 µg/ml streptomycin as previously described [44]. Transfection with the human ATX-pcDNA-GFP construct and peGFP-N1 (BD Clontech, Germany) construct was performed by Amaxa Nucleofector electroporation (Amaxa Biosystems, Germany) and revealed nearly 90% green fluorescent cells in both cell lines.

Primary leptomeningeal cell culture and subcellular localization. Cerebrum was prepared from P1 C56BL/6 mouse pups and the meninges, specifically the pia mater and arachnoid, were carefully stripped off and washed in DMEM (4.5 g/l glucose, 200 mM glutamine, pyruvate), containing 10% fetal calf serum and 100 U/ml penicillin/streptomycin to remove glial tissue. Following 15 min of trypsin (1.25%) incubation, digestion was stopped by adding the same volume of culture medium (DMEM containing 4.5 g/l glucose, 200 mM glutamine, pyruvate, 10% fetal calf serum; and 100 U/ml penicillin/streptomycin) to the tube. The cells were re-collected by centrifugation and resuspended in low volume. Dissociation was carefully performed by fire-polished Pasteur pipette resuspension five to ten times, without air bubble aspiration. The dissociated leptomeningeal cells were plated on collagen-G (Biochrom, Berlin, Germany)-coated glass slides or poly-L-lysine (5 µg/ml)-coated dishes. Once the cells became confluent, they were harvested with 0.25% (w/v) trypsin for 10 min at 37 °C, resuspended with a fire-polished Pasteur pipette, and replated in culture medium in low density (1000 cells/cm²).

For immunocytochemical analysis, cultures were fixed in 4% PFA, containing 3% BSA for 20 min at room temperature. Cells were then washed three times in PBS containing 3% BSA and further processed for antibody incubation (overnight at 4 °C). The following antibodies were used: anti-ATX (rat monoclonal clone 4F1), anti-fibronectin (Sigma, Germany), anti-GFAP (DAKO, USA), and anti-Thy1 (ICN, Germany). Alexa 488 and 594 secondary antibodies (Molecular Probes, The Netherlands) in 1 : 800 dilution were used. Over 90% of the cultured cells were immunopositive for fibronectin (a marker for leptomeningeal cells) and fewer than 5% of the cells were GFAP positive (a marker for astrocytes).

For subcellular localization of ATX, we used anti-clathrin to detect coated membrane vesicles (Abcam, UK) and anti-EEA1 mAb for early endosomes (Abcam, UK). Single fluorescence sections were taken with a Leica DM LB microscope. Digital data were processed with MetaVue 4.62 software.

Preparation and purification of oligodendrocyte precursor cells. Primary mixed glial cultures were prepared

from the cerebral hemispheres of P0–P2 Sprague-Dawley rat pups from which the meninges had been stripped. After 10–14 days, the oligodendrocyte precursor cells (OPCs) were isolated on the basis of differential adherence [45, 46]. Microglia were removed by brief mechanical shaking (1 h, 260 rpm, 37 °C); next, the OPCs were detached by continued shaking (18 h, 260 rpm, 37 °C). Following a short differential adhesion step in a bacterial dish (20 min, 37 °C), the OPCs were seeded with a density of 2×10^4–5×10^4 cells/cm^2 on culture dishes coated with poly-D-lysine. To maintain the cells, proliferating growth factors PDGF-AA and FGF were added daily. To start the differentiation process, the OPCs were cultured in SATO medium + 0.5% FCS, which was changed every third day. Cells were kept in differentiation medium for 9 days (CNP+ 95%, MBP+ 55–60%).

Preparation and purification of astrocytes and microglial cells. For astrocyte and microglial preparation, cerebrum from C56BL/6 mouse pups aged P1–P3 was prepared. The pia mater and arachnoid meninges were carefully removed and the cerebrum washed in DMEM (4.5 g/l glucose, 200 mM glutamine, pyruvate) containing 10% fetal calf serum and 100 U/ml penicillin/streptomycin. Following careful homogenization with a fire-polished Pasteur pipette, a 10-min trypsin/DNase (1.25%/2 U) incubation followed, and digestion was stopped by adding the same volume of culture medium (DMEM containing 4.5 g/l glucose, 200 mM glutamine, pyrovate, 10% fetal calf serum, and 100 U/ml penicillin/streptomycin) to the tube. Dissociated astrocytes were plated on poly-L-lysine (10 µg/ml)-coated dishes. Every third day in culture, the dishes were shaken for 10 min at 37 °C and afterwards rinsed three times with warm PBS to remove microglial cells. They were then resuspended with a fire-polished Pasteur pipette, and replated in culture medium at low density. The suspended microglial cells were collected and replated in astroglial culture medium containing 2% fetal calf serum.

For immunocytochemical analysis, low-density cultures (1000 cells/cm²) were fixed in 4% PFA containing 3% BSA, for 20 min at room temperature. The cells were then washed three times in PBS/BSA, permeabilized with 0.1% Triton X-100 for 5 min and further processed for antibody incubation (for details, see *Primary leptomeningeal cell preparation* above).

Results

Developmental regulation of ATX. As a first step, we investigated ATX mRNA expression in the embryonic and postnatal brain. At embryonic day 17 (E17), ATX transcripts were found in the subventricular zones of all ventricles (Fig. 1). Additionally, ATX mRNA expression was located in white matter structures such as the anterior commissure (Fig. 1a). After birth, ATX mRNA hybridization signals declined in the subventricular zones, whereas signals remained high in white matter regions such as the anterior commissure, fimbria fornix and arbor vitae of the cerebellum (Fig. 1a). Neuronal cell layers such as in the cortex and hippocampus were almost devoid of any ATX mRNA signals. Furthermore, quantitative RT-PCR analysis showed increased ATX transcripts in the first 2 postnatal weeks, which is also the time myelination takes place (Fig. 1b). Interestingly, ATX expression resembled the same transcriptional regulation as that of the LPA receptor EDG2/LPA$_1$ (Fig. 1b). Along with the white matter regions, the choroid plexus showed the strongest hybridization intensity, even in the adult brain (Fig. 1a). We then confirmed these findings, using a biochemical approach. First, we proved the specificity of the anti-ATX mAb (4F1) by blotting total lysates from ATX-GFP-expressing COS-7 cells and probing the membranes with our anti-ATX mAb or an commercially available anti-GFP antibody (Fig. 1c). A clear single band was detected with the anti-ATX antibody used, which corresponded to the band detected with the anti-GFP antibody (Fig. 1c). We performed immunoblots from total protein extracts from distinct adult rat brain areas, and the results indicated that white matter (from the corpus callosum) and the spinal cord were highly rich in ATX protein, whereas neuron-rich areas such as the cortex, hippocampus and cerebellar cortex showed much weaker levels of ATX expression (Fig. 1c).

Cellular and subcellular distribution of ATX. Since the expression pattern of the ATX transcripts and protein was distributed in brain regions known as sites of oligodendroglial residence [47], we next tested ATX expression on the cellular level in adult rat brain tissue. Double immunocytochemical analysis revealed that OLCs (CNPase-positive), which can be found in regions of the fimbria fornix, corpus callosum, and anterior commissure were immunopositive for ATX (Fig. 2a). Interestingly, not every CNPase-positive cell was ATX positive, whereas almost all ATX-positive cells showed CNPase staining. Testing with more stage-specific markers [48] showed that ATX was codistributed with OPC markers including NG2 (Fig. 2b), A2B5 (Fig. 2c) and O4 (data not shown). In contrast, CC1-expressing mature oligodendrocytes were negative for ATX (Fig. 2d). Within the OPCs, ATX expression appeared scattered in vesicle-like structures and was not associated with the plasma membrane. Similarly, ATX expression was also detected in cultured immature oligodendrocytes *in vitro* (Fig. 2f). These data (summarized in Fig. 2e) indicate that ATX expression commences prior to the onset of myelin protein expression and myelination in the brain [47, 49, 50].

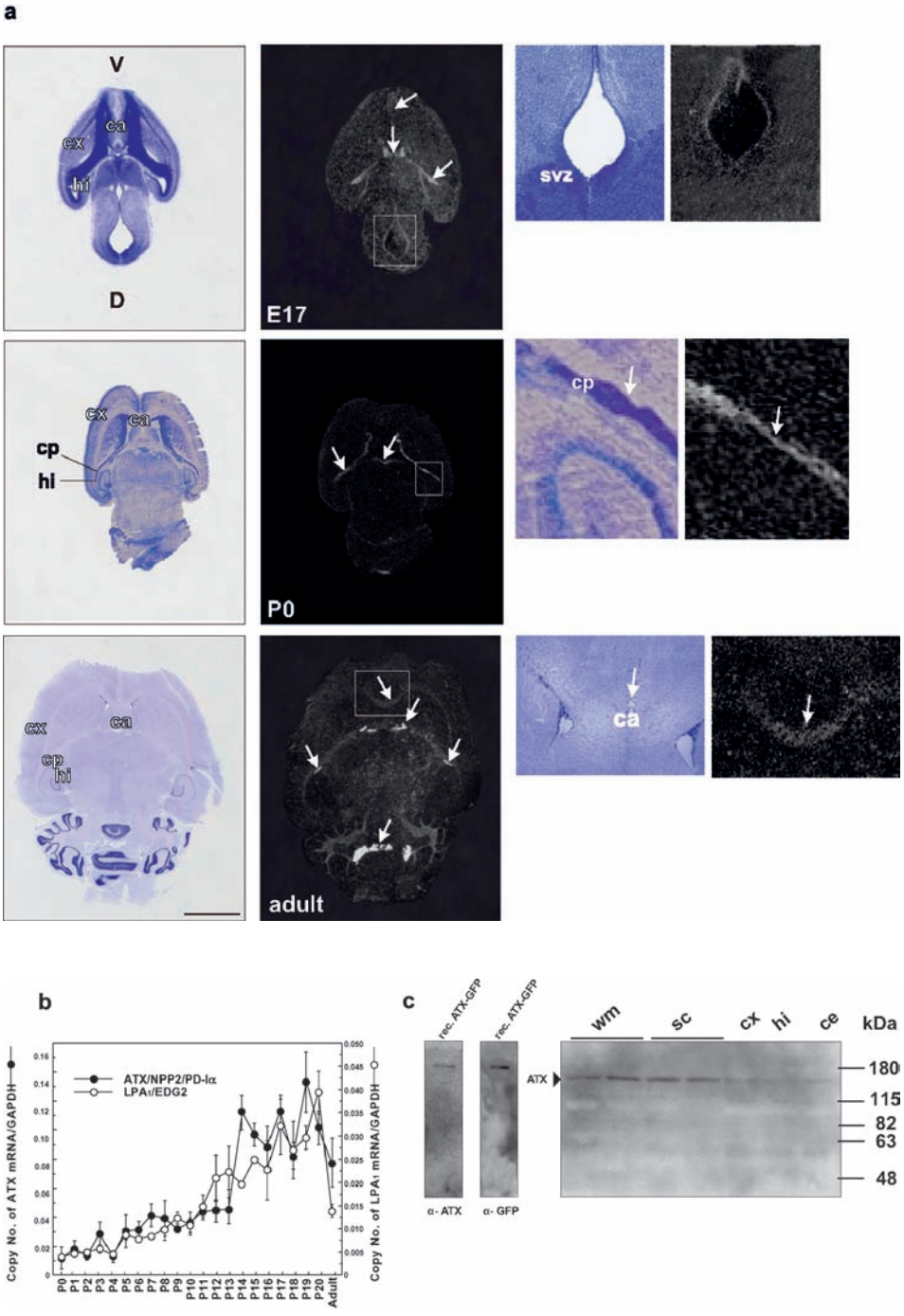

Figure 1. Developmental regulation of autotaxin (ATX) mRNA expression in the brain. (*a*) *In situ* hybridization analysis of *ATX/NPP-2/PD-1a* mRNA in horizontal rat brain sections of embryonic day 17 (E17), newborn (P0), and adult. Images on the left represent the same hybridized brain sections counterstained with toluidine blue. At various embryonic stages, ATX mRNA is expressed in the subventricular zones (boxed area), the cerebellar neuroepithelium of the 4th ventricle, the choroid plexus, and the anterior commissure. During postnatal development and in the adult, ATX mRNA is found in the choroid plexus, white matter such as the fornix, commissure anterior and arbor vitae, and in the subventricular zone. Arrows indicate choroid plexus structures in the brain. Note that for technical reasons the dura mater and arachnoid had been removed (see *Material & Methods* above). Scale bar represents 430 µm. (*b*) mRNA expression regulation of ATX and LPA_1 (EDG2) in the developing brain analyzed by quantitative RT-PCR. The number of transcripts was quantified and each sample normalized on the basis of GAPDH content. All determinations were done in triplicate. Each bar represents the mean ± SEM of the triplicate. (*c*) Recombined ATX-green fluorescent protein (GFP) served as a specificity control for the ATX mAb. The same blot was first probed with an α-ATX mAb, stripped, and reprobed with an α-GFP antibody. ATX detection by immunoblotting of total protein extracts from distinct adult rat brain areas, white matter (wm, from corpus callosum), spinal cord (sc), cortex (cx), hippocampus (hi), and cerebellum (ce). Further abbreviations: ca, commissure anterior; cp, choroid plexus; svz, subventricular zone; V, ventral; D, dorsal.

We further found that leptomeningeal and choroid plexus epithelial and ependymal cells strongly express ATX (Fig. 3a, b). In contrast, neurons and astrocytes were negative for ATX staining (Fig. 3a). The fact that leptomeningeal cells *in vivo* express ATX may mean they are the cellular source of ATX and LPA found in cerebrospinal fluid [51]. In accordance with previous descriptions of ATX as a secreted enzyme, we also found ATX located in intracellular vesicles but not in the plasma membrane (Fig. 2, 3) [21, 31, 32].

Finally, we compared the subcellular distribution of ATX in transfected HEK 293 and COS-7 cells. As previously described, catalytically active ATX fused to GFP was mainly found in intracellular vesicle-like structures rather than at the plasma membrane or nuclear compartment (Fig. 3c) [31]. We also examined the expression of endogenous ATX mRNA using RT-PCR analysis, and found that HEK293 cells but not COS-7 cells expressed ATX endogenously at high levels (Fig. 3d). Therefore, we used these two cell types and compared the distribution of overexpressed ATX in COS-7 and HEK293 cells (Fig. 3c). Expressing full-length ATX C-terminally fused to GFP in COS-7 cells displayed essentially the same scattered dot-like appearance as found in ATX-GFP expressing HEK 293 cells (Fig. 3c). Here, ATX was distributed in vesicle-like structures of different sizes within the cytoplasm, whereas the nuclei and plasma membrane were almost free of GFP signals. Previously, we had shown that HEK 293 cells secrete ATX into the medium when overexpressed [31]. Therefore, we now used COS-7 cells, which do not endogenously express ATX, and followed its trafficking route. We were able to clearly detect ATX in the conditioned medium of transfected COS-7 cells (Fig. 3).

Since it has been suggested that ATX and LPA in the cerebrospinal fluid, at least *in vitro*, both derive from leptomeningeal cells [51], we then examined ATX expression in cultured primary leptomeningeal cells. We found that the fibronectin-positive leptomeningeal cells were highly immunopositive for ATX and that the latter is distributed in cytoplasmic vesicles (Fig. 3f, g). Given their distribution pattern and round shape, we hypothesized that these structures are of exocytotic origin: membrane vesicles or secretory vesicles. Double-immunofluorescence analysis further confirmed that ATX did not colocalize with clathrin, a membrane vesicle marker for endocytosis, and was not surrounded by clathrin-positive membrane vesicles (Fig. 3f). Furthermore, ATX did not colocalize with Lamp1, a marker for late endosomes/lysosomes (data not shown); however, some ATX-positive vesicles colocalized with EEA1, a marker for early endosomes (Fig. 3g). To confirm these findings, we then used Western blotting to detect ATX. In these experiments, ATX was found in total lysates of leptomeninges as well as in the conditioned supernatants of these cells (Fig. 3h).

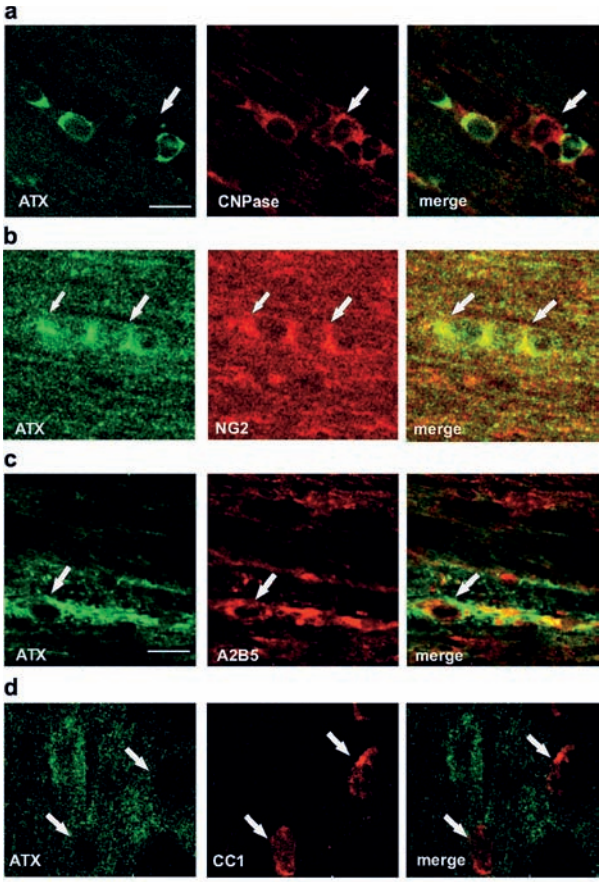

e

Antibody	Maturation stage	ATX
CNPase	all stages, strong in mature OLs	+/-
NG2	early OPCs, adult OPCs	+
A2B5	early OPCs	+
CC1	mature OLs	-

Figure 2. ATX is expressed in early and late oligodendrocyte precursor cells (OPCs). Confocal images from rat brain sections immunostained for ATX in regions of the fimbria fornix, corpus callosum, and anterior commissure (animals, n=4). (*a*) In the adult brain, ATX-immunopositive cells (green) are colocalized with the oligodendroglial marker CNPase (red). Interestingly, not every CNPase-positive cell is ATX positive (indicated by white arrows in *a*), whereas almost all ATX-positive cells show CNPase staining. Double immunostaining for ATX (green) and NG2 (red, *b*) and A2B5 (red, *c*) indicates codistribution, as highlighted by the white arrows in *b* and *c* pointing to immunopositive ATX and NG2 or A2B5 cells. ATX-positive oligodendrocytes do not colocalize with CC1 (red, *d*). Arrows in *d* indicate CC1 positive cells that are negative for ATX staining. (*e*) Table summarizes the co-immunostaining results. (*f*) ATX expression in cultured oligodendrocytes as shown by immunoblotting. Scale bar *a*, *b*, *d* 5 µm; *c* 8 µm. OLs, oligodendrocytes.

ATX is up-regulated and cell-type-specifically expressed following neurotrauma. We continued our investigation by analyzing the expression pattern of ATX in the brain after lesioning. In concordance with our *in*

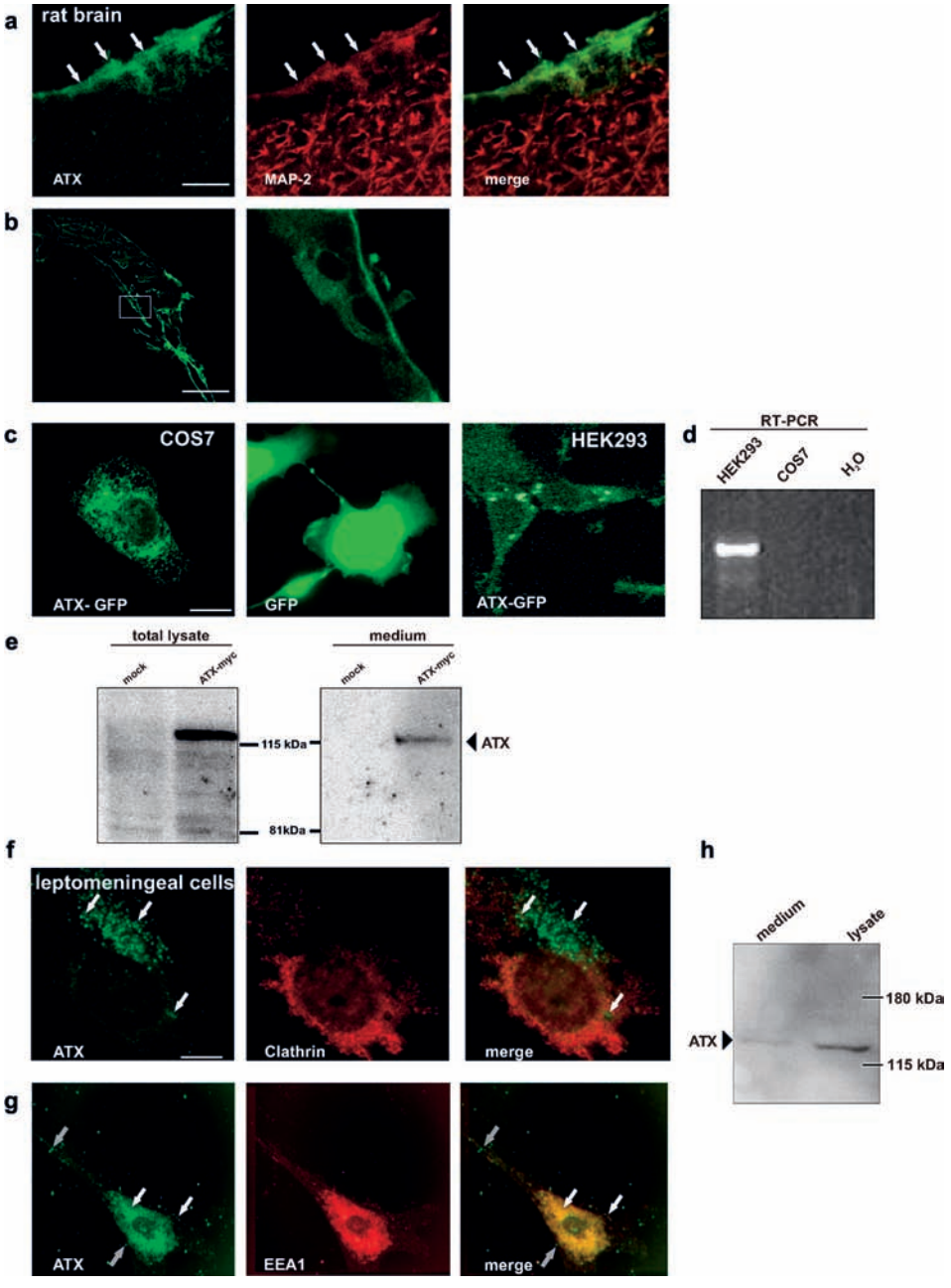

Figure 3. ATX is expressed in vesicle-like structures in leptomeningeal cells *in vivo*. (*a*) Leptomeningeal cells *in vivo* are highly immunopositive for ATX (green), whereas MAP2-positive neurons (red) do not colocalize with ATX. (*b*) Choroid plexus epithelium and ependymal epithelium *in vivo* stained for ATX. The right-hand image represents higher magnification of the boxed area in the left image. (*c*) Enzymatically active human full-length ATX C-terminally fused to GFP was expressed in COS-7 and HEK293 cells. Visualizing ATX-GFP expression on a subcellular level indicates its distribution in intracellular vesicles and endoplasmic reticulum-like structures, whereas the plasma membrane and nuclei remain unstained. Note the distribution of GFP in solely GFP-expressing cells (right) throughout all compartments, *i.e.* in nuclei and cytosol. ATX-GFP overexpression in HEK293 cells shows that the organization of ATX-containing vesicles appears in heterogeneous sizes. (*d*) RT-PCR analysis revealed that HEK293 cells express ATX endogenously, whereas COS-7 cells are negative for endogenous ATX expression. (*e*) Full-length ATX-myc fusion protein was expressed in COS-7 cells. ATX expression in cell lysates and conditioned medium was analyzed by immunoblotting with an anti-myc antibody. Expressed ATX was found in total lysates as well as in conditioned serum-free medium. Mock transfected (empty pcDNA3.1 vector) cells served as a control. (*f*) Cultured leptomeningeal cells *in vitro* show strong immunopositive staining for ATX, subsequent immunocytochemical analysis indicates no colocalization with the membrane vesicle marker clathrin (red). (*g*) Further, ATX shows localization in some cases with EEA1, a marker for early endosomes (red). (*h*) Endogenous ATX expression in cultured leptomeningeal cells found in total lysates and in conditioned serum-free medium detected by immunoblotting. Scale bar represents in *a*, 20 µm; *b*, 60 µm; *c*, 8 µm, *e*, 5 µm; *f*, 50 µm.

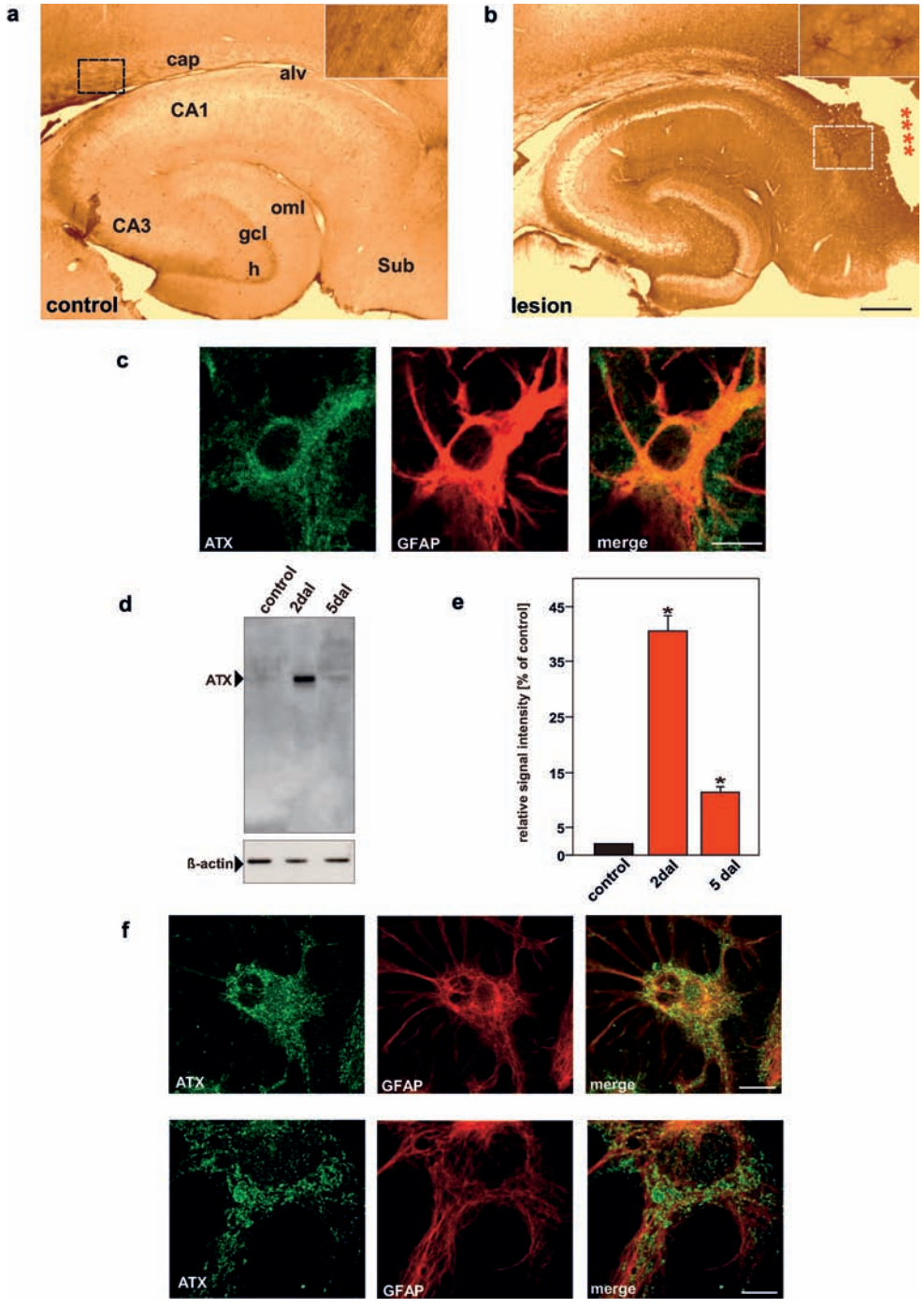

Figure 4. ATX distribution in the hippocampus following neurotrauma. Immunocytochemical analysis of ATX on adult rat brain sections (for details see *Material and methods* above, animals n=4). (*a*) In non-lesioned adult controls, ATX-immunopositive cells are located in white matter areas, such as the alveus and the fimbria. Insert represents higher magnification of the boxed area in *a* and shows an ATX-immunopositive oligodendrocyte-like cell. (*b*) At 5 days after lesion, an increased number of ATX-immunopositive cells appeared around the lesion (marked with red asterisks). Insert represents higher magnification of the boxed area in *b* and shows an ATX-immunopositive cell, which resembles an astrocytic phenotype. (*c*) Following brain lesion, ATX-immunopositive cells around the lesion resembled the stellate-like morphology of astrocytes and were almost exclusively colocalized with the astrocyte marker GFAP (red). (*d*) Immunoblots from total protein extracts of adult control and lesioned hippocampus of various survival stages. β-Actin expression levels were used as an internal control to standardize the protein amount, ensuring equal protein loading. (*e*) Quantification of immunoblots of three different experiments. Data represent three separate protein samples in each group. Statistical difference is marked with an asterisk (mean ± SD), * $p < 0.05$; Mann-Whitney U-test. (*f*) Cultured GFAP$^+$ reactive astrocytes (red) show strong colocalization with ATX immunostaining. At a higher magnification, the typically vesicle-like structures positive for ATX are visible. Scale bar: *b* 60 µm; *c* 1.2 µm; *f* upper panel 10 µm, lower panel 1 µm. cap: capsule; alv: alveus; CA1: Cornu ammonis regio superior; CA3: Cornu ammonis regio inferior; gcl: granular cell layer of the dentatus gyrus; oml: dentate outer molecular layer; h: hilus; Sub: subiculum.

situ hybridization data, ATX-immunopositive cells were located in white matter regions, such as the alveus, stratum lacunosum-moleculare, and in cortical layer IV in adult non-lesioned control animals (Fig. 4a). Following traumatic brain injury, ATX was massively up-regulated at the lesion site and in the denervated area after 2 days (Fig. 4b–e). This lesion-induced up-regulation was restricted to the site of incision and to the area of axonal degeneration, whereas non-affected brain regions did not show any altered expression. The massive up-regulation (~20-fold) of ATX peaked after 2 days post lesion and remained high for 5 days (Fig. 4d). Further, double immunocytochemistry showed that many ATX-positive cells were also GFAP positive, a marker for reactive astrocytes (Fig. 4c). Again, ATX appeared in vesicle-like structures scattered within the cytoplasm. Co-immunolabeling of ATX with markers for microglia (IB4, CD11) and for adult precursors (NG2) [52] did not indicate any double staining (data not shown). Thus, it seems that, while astrocytes do not express ATX in a detectable manner under physiological conditions, ATX expression is heavily induced in reactive astrocytes following traumatic injury to the brain. To confirm these data, we analyzed endogenous ATX expression in primary astrocytes *in vitro*. Recent gene-expression analysis revealed that these cultured astrocytes, when isolated from postnatal brains, resemble the cellular and molecular properties of reactive astrocytes *in vivo* [53]. In our study, astrocytes *in vitro* were highly immunopositive for ATX and also showed a dot-like distribution of ATX throughout the cytoplasm, comparable to what is seen *in vivo* (Fig. 4f).

Discussion

This is to our knowledge the first systematic *in vivo* study of the cellular distribution and cell-type-specific regulation of the LPA-generating enzyme ATX in the brain. During embryonic brain development, ATX is mainly evident in the circumventricular and subventricular zones and in white matter areas such as the corpus callosum, fimbria-fornix and anterior commissure. In postnatal stages and in the adult brain, ATX expression declines in the subventricular zones. In concordance with our findings, previous studies have shown that ATX transcripts are also located in other white matter areas such as the optic nerve and spinal cord of postnatal rats [36, 37].

Cellular distribution of ATX in the brain. We found *in vivo* that oligodendrocytes, choroid plexus epithelial cells and leptomeningeal cells express ATX in the brain under normal conditions, but that neurons, astrocytes, and microglia are immunonegative for ATX. Interestingly, ATX expression commences prior to the onset of myelination, suggesting a role in regulating the initial stages of differentiation and myelin formation. This is further supported by the discovery that the early OPCs, positive for NG2 and A2B5, also express ATX, and that ATX-expressing cells do not colocalize with CC1, a marker for mature, myelinating oligodendrocytes. Consistent with these observations, expression of the LPA receptor LPA_1 in oligodendrocytes correlates temporally with the process of myelination [9, 54]. Additionally, the temporal development of ATX expression in the developing brain is quite similar to that of LPA_1 (Fig. 1b). As has been found and characterized previously, ATX stimulates the cell motility of many cell types, including tumor cells [19, 55, 56]. Previous studies show that ATX-dependent cell motility stimulation can be attributed to the production of LPA and potentially S1P [41, 57–59]. Thus, it is not surprising that both phospholipids exist in the brain at relatively high concentrations [60, 61]. However, the group of Drs. B. Fuss and W. B. Macklin report that ATX also has counteradhesive effects on the N19 cell line and on $O4^+$ oligodendrocytes *in vitro* [37]. The counteradhesive effects reported *in vitro* were mainly found on extracellular matrix (ECM) proteins fibronectin, laminin2/merosin but not on poly-L-lysine [37]. Moreover, at least in the case of the N19 cell line, ATX-dependent counteradhesive effects were blocked by pertussis toxin, indicating that G_i-protein coupled receptor signaling is required in these processes. Interestingly, the observed effects identified a C-terminal oligodendrocyte-remodeling domain in ATX and that counteradhesion did not depend on the catalytic domain of ATX [37, 62]. Thus, these findings suggest additional, LPA-independent functions of ATX, and propose ATX as a multifunctional protein. This might be supported by the rather complex phenotype found in ATX-deficient mice. Homozygous ATX deletion leads to embryonic lethality at day 9.5–10.5 with massive neural tube defects and absence of mature vessels, which has not been found in LPA-receptor-deficient mice [35, 36]. The $ATX^{-/-}$ phenotype might, therefore, be caused by disruption of an as yet unidentified LPA-receptor-signaling pathway or by its function, independently of the catalytic domain.

ATX expression in neuropathological conditions. Lysophospholipids in general and LPA in particular can affect most neural cell types, impacting axonal and dendritic morphology [5, 43], neuronal apoptosis [63], neural precursor cell survival [4], process retraction in OLCs [64], hypertrophy of astrocytes [65], microglial activation and migration [66]. Furthermore, LPA levels are increased during pathological conditions in the brain, such as in cerebral ischemia, and following disruption of the blood-brain barrier [67–69]. Moreover,

LPA can induce hyperphosphorylation of the Tau protein [70] and ATX mRNA was found to be elevated in brains with Alzheimer's disease [71]. Additionally, high concentrations of intrathecally applied LPA cause receptor-dependent demyelination in dorsal root ganglia and PKCγ up-regulation in the spinal cord [72]. The data on LPA-induced demyelination in dorsal roots and alterations in oligodendrocyte function are further supported by a study in humans suffering from multiple sclerosis (MS), a demyelinating disease of unknown cause. In an investigation using a proteomic approach, it has been reported that 103 protein spots were uniquely present in MS samples but not in samples from patients with non-MS-related disorders [73]. One of these unique protein spots appeared to be ATX [73]. In contrast, it has been reported that ATX mRNA slightly decreases (20% reduction) at the onset of clinical symptoms in experimental autoimmune encephalomyelitis in mice, an animal model for MS [36]. However, since ATX and LPA are also present in cerebrospinal fluid under physiological conditions, as confirmed in rodents and dogs [51], further studies are required to more precisely define the transcriptional and translational regulation of ATX and its consequences in autoimmune diseases such as MS. We propose that LPA may affect neural regeneration in two ways, with consequences for myelination and axon growth: (1) LPA hampers and remodels neurite outgrowth and affects oligodendrocyte function; and (2) LPA modulates OPC-ECM interaction and cell survival.

Following brain lesion, ATX is highly up-regulated in the affected areas. This up-regulation is restricted solely to astrocytes. In a recent study, Corcoran et al. [74] provided compelling evidence that ATX expression is driven by the transcription factor NF-κB, a transcription factor also activated following brain lesioning [75]. In light of this, our finding that reactive astrocytes up-regulate ATX is especially interesting. These data suggest that, following injury to the brain, an increase in expression of ATX, which is intrinsically generated by reactive astrocytes, leads to increased LPA concentrations. Astrocytes represent a cell population that exhibits a dual nature with respect to regeneration. These cells are implicated in the chemo-attraction of cells in the immune system and neuronal precursors, as well as having counter-adhesive effects on neuroregeneration and axon growth [76]. In effect, two hallmarks of reactive astrogliosis (scar formation by reactive astrocytes) can be induced by LPA itself: hypertrophy of astrocytes and stress fiber formation [65]. This may indicate an autoregulation loop of astrocytic activation, in which astrocytes up-regulate the LPA-generating enzyme ATX and become activated by its metabolite LPA, while increased amounts of the metabolite inhibit the catalytic activity of ATX [31]. In a previous study by Stefan and colleagues [77], it was shown that ATX mRNA expression is strictly growth-related in the liver. The authors further reported that, following hepatectomy in rats, ATX mRNA decreases within 24 h, and that this effect could also be induced by administration of the translational inhibitor cycloheximide, suggesting that ATX levels are controlled by an RNA-stabilizing protein [77]. Furthermore, it has been shown that ATX, along with LPA_1, is highly expressed in glioma cell lines and contributes to cell motility [23]. In summary, these data indicate the involvement and regulation of ATX in different neuropathological conditions, although the molecular mechanisms of ATX transcription and translation remain unknown.

In conclusion, our report demonstrates the presence of the LPA-generating enzyme ATX in the brain and its up-regulation after neurotrauma, which may modulate the neuronal regeneration capacity. Since conventional gene disruption of ATX leads to embryonic lethality, the generation of inducible and cell-type specific, *i.e.* leptomeningeal, reactive astrocytes and oligodendrocyte-specific ATX knockouts may provide further insights into the role of ATX in the brain. Thus, further studies that include interfering approaches in ATX signaling (*e.g.* on the level of LPA receptors and the pharmacological and genetic inhibition of ATX and LPA signaling) are needed, which will help to unravel the mechanisms and role of ATX in the brain during development and following injury to the brain.

Acknowledgements. The authors thank Bettina Brokowski, Rike Dannenberg, Tobias Thiele and Jan Csupor for their expert technical support; and Sabine Lewandowski for her help with digital image processing. Kimberly Rosegger and Ari Liebkowsky are acknowledged for editorial assistance on the manuscript. This study was supported by the Deutsche Forschungsgemeinschaft (DFG): SFB 515/A5 (to R. N. and A.U.B.), DFG SA 1041/4-1 (to N.E.S.), and the Charité Medical Research Foundation (to A.U.B.). N. E. Savaskan is a fellow of the Human Frontier Science Program (HFSP).

1 Mills, G. B. and Moolenaar, W. H. (2003) The emerging role of lysophosphatidic acid in cancer. Nat. Rev. Cancer 3, 582–591.
2 Tigyi, G. and Parrill, A. L. (2003) Molecular mechanisms of lysophosphatidic acid action. Prog. Lipid Res. 42, 498–526.
3 Moolenaar, W. H., van Meeteren, L. A. and Giepmans, B. N. (2004) The ins and outs of lysophosphatidic acid signaling. Bioessays 26, 870–881.
4 Kingsbury, M. A., Rehen, S. K., Contos, J. J., Higgins, C. M. and Chun, J. (2003) Non-proliferative effects of lysophosphatidic acid enhance cortical growth and folding. Nat. Neurosci. 6, 1292–1299.
5 Fukushima, N., Weiner, J. A. and Chun, J. (2000) Lysophosphatidic acid (LPA) is a novel extracellular regulator of cortical neuroblast morphology. Dev. Biol. 228, 6–18.
6 Anliker, B. and Chun, J. (2004) Lysophospholipid G protein-coupled receptors. J. Biol. Chem. 279, 20555–20558.
7 Ishii, I., Fukushima, N., Ye, X. and Chun, J. (2004) Lysophospholipid receptors: signaling and biology. Annu. Rev. Biochem. 73, 321–354.
8 Tokumura, A., Harada, K., Fukuzawa, K. and Tsukatani, H. (1986) Involvement of lysophospholipase D in the production of lysophosphatidic acid in rat plasma. Biochim. Biophys. Acta 875, 31–38.

9 Fukushima, N. and Chun, J. (2001) The LPA receptors. Prostaglandins Other Lipid Mediat. 64, 21–32.
10 Xie, Y., Gibbs, T. C., Mukhin, Y. V. and Meier, K. E. (2002) Role for 18 : 1 lysophosphatidic acid as an autocrine mediator in prostate cancer cells. J. Biol. Chem. 277, 32516–32526.
11 Hama, K., Bandoh, K., Kakehi, Y., Aoki, J. and Arai, H. (2002) Lysophosphatidic acid (LPA) receptors are activated differentially by biological fluids: possible role of LPA-binding proteins in activation of LPA receptors. FEBS Lett. 523, 187–192.
12 Sugiura, T., Nakane, S., Kishimoto, S., Waku, K., Yoshioka, Y. and Tokumura, A. (2002) Lysophosphatidic acid, a growth factor-like lipid, in the saliva. J. Lipid Res. 43, 2049–2055.
13 Aoki, J. (2004) Mechanisms of lysophosphatidic acid production. Semin. Cell Dev. Biol. 15, 477–489.
14 Xu, Y., Gaudette, D. C., Boynton, J. D., Frankel, A., Fang, X. J., Sharma, A., Hurteau, J., Casey, G., Goodbody, A., Mellors, A. et al. (1995) Characterization of an ovarian cancer activating factor in ascites from ovarian cancer patients. Clin. Cancer Res. 1, 1223–1232.
15 Siess, W., Zangl, K. J., Essler, M., Bauer, M., Brandl, R., Corrinth, C., Bittman, R., Tigyi, G. and Aepfelbacher, M. (1999) Lysophosphatidic acid mediates the rapid activation of platelets and endothelial cells by mildly oxidized low density lipoprotein and accumulates in human atherosclerotic lesions. Proc. Natl. Acad. Sci. USA 96, 6931–6936.
16 Kusaka, S., Kapousta-Bruneau, N., Green, D. G. and Puro, D. G. (1998) Serum-induced changes in the physiology of mammalian retinal glial cells: role of lysophosphatidic acid. J. Physiol. 506, 445–458.
17 Tokumura, A., Majima, E., Kariya, Y., Tominaga, K., Kogure, K., Yasuda, K. and Fukuzawa, K. (2002) Identification of human plasma lysophospholipase D, a lysophosphatidic acid-producing enzyme, as autotaxin, a multifunctional phosphodiesterase. J. Biol. Chem. 277, 39436–39442.
18 Umezu-Goto, M., Kishi, Y., Taira, A., Hama, K., Dohmae, N., Takio, K., Yamori, T., Mills, G. B., Inoue, K., Aoki, J. and Arai, H. (2002) Autotaxin has lysophospholipase D activity leading to tumor cell growth and motility by lysophosphatidic acid production. J. Cell Biol. 158, 227–233.
19 Stracke, M. L., Krutzsch, H. C., Unsworth, E. J., Arestad, A., Cioce, V., Schiffmann, E. and Liotta, L. A. (1992) Identification, purification, and partial sequence analysis of autotaxin, a novel motility-stimulating protein. J. Biol. Chem. 267, 2524–2529.
20 Nam, S. W., Clair, T., Campo, C. K., Lee, H. Y., Liotta, L. A. and Stracke, M. L. (2000) Autotaxin (ATX), a potent tumor motogen, augments invasive and metastatic potential of ras-transformed cells. Oncogene 19, 241–247.
21 Jansen, S., Stefan, C., Creemers, J. W. M., Waelkens, E., Van Eynde, A., Stalmans, W. and Bollen, M. (2005) Proteolytic maturation and activation of autotaxin (NPP2), a secreted metastasis-enhancing lysophospholipase D. J. Cell Sci. 118, 3081–3089.
22 Baumforth, K. R., Flavell, J. R., Reynolds, G. M., Davies, G., Pettit, T. R., Wei, W., Morgan, S., Stankovic, T., Kishi, Y., Arai, H., Nowakova, M., Pratt, G., Aoki, J., Wakelam, M. J., Young, L. S. and Murray, P. G. (2005) Induction of autotaxin by the Epstein-Barr virus promotes the growth and survival of Hodgkin lymphoma cells. Blood 106, 2138–2146.
23 Kishi, Y., Okudaira, S., Tanaka, M., Hama, K., Shida, D., Kitayama, J., Yamori, T., Aoki, J., Fujimaki, T. and Arai, H. (2006) Autotaxin is overexpressed in glioblastoma multiforme and contributes to cell motility of glioblastoma by converting lysophosphatidylcholine to lysophosphatidic acid. J. Biol. Chem. 281, 17492–17500.
24 Goding, J. W., Terkeltaub, R., Maurice, M., Deterre, P., Sali, A. and Belli, S. I. (1998) Ecto-phosphodiesterase/pyrophosphatase of lymphocytes and non-lymphoid cells: structure and function of the PC-1 family. Immunol. Rev. 161, 11–26.
25 Bollen, M., Gijsbers, R., Ceulemans, H., Stalmans, W. and Stefan, C. (2000) Nucleotide pyrophosphatases/phosphodiesterases on the move. Crit. Rev. Biochem. Mol. Biol. 35, 393–432.
26 Stefan, C., Jansen, S. and Bollen, M. (2005) NPP-type ectophosphodiesterases: unity in diversity. Trends Biochem. Sci. 30, 542–550.
27 Ohe, Y., Ohnishi, H., Okazawa, H., Tomizawa, K., Kobayashi, H., Okawa, K. and Matozaki, T. (2003) Characterization of nucleotide pyrophosphatase-5 as an oligomannosidic glycoprotein in rat brain. Biochem. Biophys. Res. Commun. 308, 719–725.
28 Sakagami, H., Aoki, J., Natori, Y., Nishikawa, K., Kakehi, Y., Natori, Y. and Arai, H. (2005) Biochemical and molecular characterization of a novel choline-specific glycerophosphodiester phosphodiesterase belonging to the nucleotide pyrophosphatase/phosphodiesterase family. J. Biol. Chem. 280, 23084–23093.
29 Duan, R. D., Bergman, T., Xu, N., Wu, J., Cheng, Y., Duan, J., Nelander, S., Palmberg, C. and Nilsson, A. (2003) Identification of human intestinal alkaline sphingomyelinase as a novel ecto-enzyme related to the nucleotide phosphodiesterase family. J. Biol. Chem. 278, 38528–38536.
30 Goding, J. W., Grobben, B. and Slegers, H. (2003) Physiological and pathophysiological functions of the ecto-nucleotide pyrophosphatase/phosphodiesterase family. Biochim. Biophys. Acta 1638, 1–19.
31 van Meeteren, L. A., Ruurs, P., Christodoulou, E., Goding, J. W., Takakusa, H., Kikuchi, K., Perrakis, A., Nagano, T. and Moolenaar, W. H. (2005) Inhibition of autotaxin by lysophosphatidic acid and sphingosine-1-phosphate. J. Biol. Chem. 280, 21155–21161.
32 Koike, S., Keino-Masu, K., Ohto, T. and Masu, M. (2006) The N-terminal hydrophobic sequence of autotaxin (ENPP2) functions as a signal peptide. Genes Cells 11, 133–142.
33 Tanaka, M., Okudaira, S., Kishi, Y., Ohkawa, R., Iseki, S., Ota, M., Noji, S., Yatomi, Y., Aoki, J. and Arai, H. (2006) Autotaxin stabilizes blood vessels and is required for embryonic vasculature by producing lysophosphatidic Acid. J. Biol. Chem. 281, 25822–25830.
34 van Meeteren, L. A., Ruurs, P., Stortelers, C., Bouwman, P., van Rooijen, M. A., Pradere, J. P., Pettit, T. R., Wakelam, M. J., Saulnier-Blache, J. S., Mummery, C. L., Moolenaar, W. H. and Jonkers, J. (2006) Autotaxin, a secreted lysophospholipase D, is essential for blood vessel formation during development. Mol. Cell Biol. 26, 5015–5022.
35 Bachner, D., Ahrens, M., Betat, N., Schroder, D. and Gross, G. (1999) Developmental expression analysis of murine autotaxin (ATX). Mech. Dev. 84, 121–125.
36 Fuss, B., Baba, H., Phan, T., Tuohy, V. K. and Macklin, W. B. (1997) Phosphodiesterase I, a novel adhesion molecule and/or cytokine involved in oligodendrocyte function. J. Neurosci. 17, 9095–9103.
37 Fox, M. A., Colello, R. J., Macklin, W. B. and Fuss, B. (2003) Phosphodiesterase-I alpha/autotaxin: a counteradhesive protein expressed by oligodendrocytes during onset of myelination. Mol. Cell. Neurosci. 23, 507–519.
38 Narita, M., Goji, J., Nakamura, H. and Sano, K. (1994) Molecular cloning, expression, and localization of a brain-specific phosphodiesterase I/nucleotide pyrophosphatase (PD-I alpha) from rat brain. J. Biol. Chem. 269, 28235–28242.
39 Dennis, J., Nogaroli, L. and Fuss, B. (2005) Phosphodiesterase-Ialpha/autotaxin (PD-Ialpha/ATX): a multifunctional protein involved in central nervous system development and disease. J. Neurosci. Res. 82, 737–742.
40 Tokumura, A., Fujimoto, H., Yoshimoto, O., Nishioka, Y., Miyake, M. and Fukuzawa, K. (1999) Production of lysophospha-

tidic acid by lysophospholipase D in incubated plasma of spontaneously hypertensive rats and Wistar Kyoto rats. Life Sci. 65, 245–253.
41 Clair, T., Aoki, J., Koh, E., Bandle, R. W., Nam, S. W., Ptaszynska, M. M., Mills, G. B., Schiffmann, E., Liotta, L. A. and Stracke, M. L. (2003) Autotaxin hydrolyzes sphingosylphosphorylcholine to produce the regulator of migration, sphingosine-1-phosphate. Cancer Res. 63, 5446–5453.
42 Paxinos, G., Watson, C., Pennisi, M. and Topple, A. (1985) Bregma, lambda and the interaural midpoint in stereotaxic surgery with rats of different sex, strain and weight. J. Neurosci. Methods 13, 139–143.
43 Brauer, A. U., Savaskan, N. E., Plaschke, M., Ninnemann, O. and Nitsch, R. (2003) Cholecystokinin expression after hippocampal deafferentiation: molecular evidence revealed by differential display-reverse transcription-polymerase chain reaction. Neuroscience 121, 111–121.
44 Brauer, A. U., Nitsch, R. and Savaskan, N. E. (2004) Identification of macrophage/microglia activation factor (MAF) associated with late endosomes/lysosomes in microglial cells. FEBS Lett. 563, 41–48.
45 Colognato, H., Ramachandrappa, S., Olsen, I. M. and ffrench-Constant, C. (2004) Integrins direct Src family kinases to regulate distinct phases of oligodendrocyte development. J. Cell Biol. 167, 365–375.
46 Mccarthy, K. D. and Devellis, J. (1980) Preparation of separate astroglial and oligodendroglial cell-cultures from rat cerebral tissue. J. Cell Biol. 85, 890–902.
47 Reynolds, R. and Wilkin, G. P. (1988) Development of macroglial cells in rat cerebellum. 2. An *In situ* immunohistochemical study of oligodendroglial lineage from precursor to mature myelinating cell. Development 102, 409–425.
48 Ness, J. K., Valentino, M., Mciver, S. R. and Goldberg, M. P. (2005) Identification of oligodendrocytes in experimental disease models. Glia 50, 321–328.
49 Meier, S., Brauer, A. U., Heimrich, B., Schwab, M. E., Nitsch, R. and Savaskan, N. E. (2003) Molecular analysis of Nogo expression in the hippocampus during development and following lesion and seizure. FASEB J. 17, 1153–1155.
50 Meier, S., Brauer, A. U., Heimrich, B., Nitsch, R. and Savaskan, N. E. (2004) Myelination in the hippocampus during development and following lesion. Cell. Mol. Life Sci. 61, 1082–1094.
51 Sato, K., Malchinkhuu, E., Muraki, T., Ishikawa, K., Hayashi, K., Tosaka, M., Mochiduki, A., Inoue, K., Tomura, H., Mogi, C., Nochi, H., Tamoto, K. and Okajima, F. (2005) Identification of autotaxin as a neurite retraction-inducing factor of PC12 cells in cerebrospinal fluid and its possible sources. J. Neurochem. 92, 904–914.
52 Dehn, D., Burbach, G. J., Schafer, R. and Deller, T. (2006) NG2 upregulation in the denervated rat fascia dentata following unilateral entorhinal cortex lesion. Glia 53, 491–500.
53 Wu, V. W., Nishiyama, N. and Schwartz, J. P. (1998) A culture model of reactive astrocytes: increased nerve growth factor synthesis and reexpression of cytokine responsiveness. J. Neurochem. 71, 749–756.
54 Weiner, J. A., Hecht, J. H. and Chun, J. (1998) Lysophosphatidic acid receptor gene vzg-1/lp(A1)/edg-2 is expressed by mature oligodendrocytes during myelination in the postnatal murine brain. J. Comp. Neurol. 398, 587–598.
55 Lee, H. Y., Bae, G. U., Jung, I. D., Lee, J. S., Kim, Y. K., Noh, S. H., Stracke, M. L., Park, C. G., Lee, H. W. and Han, J. W. (2002) Autotaxin promotes motility via G protein-coupled phosphoinositide 3-kinase gamma in human melanoma cells. FEBS Lett. 515, 137–140.
56 Hama, K., Aoki, J., Fukaya, M., Kishi, Y., Sakai, T. and Suzuki, R. (2004) Lysophosphatidic acid and autotaxin stimulate cell motility of neoplastic and non-neoplastic cells through LPA(1). J. Biol. Chem. 279, 17634–17639.
57 Lee, H. Y., Clair, T., Mulvaney, P. T., Woodhouse, E. C., Aznavoorian, S., Liotta, L. A. and Stracke, M. L. (1996) Stimulation of tumor cell motility linked to phosphodiesterase catalytic site of autotaxin. J. Biol. Chem. 271, 24408–24412.
58 Koh, E., Clair, T., Woodhouse, E. C., Schiffmann, E., Liotta, L. and Stracke, M. (2003) Site-directed mutations in the tumor-associated cytokine, autotaxin, eliminate nucleotide phosphodiesterase, lysophospholipase D, and motogenic activities. Cancer Res. 63, 2042–2045.
59 Gijsbers, R., Aoki, J., Arai, H. and Bollen, M. (2003) The hydrolysis of lysophospholipids and nucleotides by autotaxin (NPP2) involves a single catalytic site. FEBS Lett. 538, 60–64.
60 Das, A. K. and Hajra, A. K. (1989) Quantification, characterization and fatty-acid composition of lysophosphatidic acid in different rat tissues. Lipids 24, 329–333.
61 Sugiura, T., Nakane, S., Kishimoto, S., Waku, K., Yoshioka, Y., Tokumura, A. and Hanahan, D. J. (1999) Occurrence of lysophosphatidic acid and its alkyl ether-linked analog in rat brain and comparison of their biological activities toward cultured neural cells. Biochim. Biophys. Acta 1440, 194–204.
62 Fox, M. A., Alexander, J. K., Afshari, F. S., Colello, R. J. and Fuss, B. (2004) Phosphodieterase-I alpha/autotaxin and IFAK phosphorylation during controls cytoskeletal organization myelination. Mol. Cell. Neurosci. 27, 140–150.
63 Holtsberg, F. W., Steiner, M. R., Keller, J. N., Mark, R. J., Mattson, M. P. and Steiner, S. M. (1998) Lysophosphatidic acid induces necrosis and apoptosis in hippocampal neurons. J. Neurochem. 70, 66–76.
64 Dawson, J., Hotchin, N., Lax, S. and Rumsby, M. (2003) Lysophosphatidic acid induces process retraction in CG-4 line oligodendrocytes and oligodendrocyte precursor cells but not in differentiated oligodendrocytes. J. Neurochem. 87, 947–957.
65 Ramakers, G. J. and Moolenaar, W. H. (1998) Regulation of astrocyte morphology by RhoA and lysophosphatidic acid. Exp. Cell Res. 245, 252–262.
66 Schilling, T., Lehmann, F., Ruckert, B. and Eder, C. (2004) Physiological mechanisms of lysophosphatidylcholine-induced de-ramification of murine microglia. J. Physiol. (Lond) 557, 105–120.
67 Kinouchi, H., Imaizumi, S., Yoshimoto, T., Yamamoto, H. and Motomiya, M. (1990) Changes of polyphosphoinositides, lysophospholipid, and free fatty-acids in transient cerebral-ischemia of rat brain. Mol. Chem. Neuropathol. 12, 215–228.
68 Sun, G. Y., Lin, T. N., Simonyi, A., Wang, Q., Chen, J. J., Cheung, W. M., He, Y. Y., Xu, J., Sun, A. Y., Hsu, C. Y. and Sun, G. Y. (2004) Transient focal cerebral ischemia induces group IIA secretory phospholipase A2 in reactive astrocytes in rat brain. J. Neurochem. 88, 40.
69 Tigyi, G., Hong, L., Yakubu, M., Parfenova, H., Shibata, M. and Leffler, C. W. (1995) Lysophosphatidic acid alters cerebrovascular reactivity in piglets. Am. J. Physiol. 268, H2048–H2055.
70 Sayas, C. L., Moreno-Flores, M. T., Avila, J. and Wandosell, F. (1999) The neurite retraction induced by lysophosphatidic acid increases Alzheimer's disease-like Tau phosphorylation. J. Biol. Chem. 274, 37046–37052.
71 Umemura, K., Yamashita, N., Yu, X., Arima, K., Asada, T., Makifuchi, T., Murayama, S., Saito, Y., Kanamaru, K., Goto, Y., Kohsaka, S., Kanazawa, I. and Kimura, H. (2006) Autotaxin expression is enhanced in frontal cortex of Alzheimer-type dementia patients. Neurosci. Lett. 400, 97–100.
72 Inoue, M., Rashid, M. H., Fujita, R., Contos, J. J. A., Chun, J. and Ueda, H. (2004) Initiation of neuropathic pain requires lysophosphatidic acid receptor signaling. Nat. Med. 10, 712–718.
73 Hammack, B. N., Fung, K. Y., Hunsucker, S. W., Duncan, M. W., Burgoon, M. P., Owens, G. P. and Gilden, D. H. (2004) Proteomic analysis of multiple sclerosis cerebrospinal fluid. Mult. Scler. 10, 245–260.

74 Corcoran, D. L., Feingold, E., Dominick, J., Wright, M., Harnaha, J., Trucco, M., Giannoukakis, N. and Benos, P. V. (2005) Footer: A quantitative comparative genomics method for efficient recognition of cis-regulatory elements. Genome Res. 15, 840–847.

75 Acarin, L., Gonzalez, B. and Castellano, B. (2001) Triflusal posttreatment inhibits glial nuclear factor-kappaB, downregulates the glial response, and is neuroprotective in an excitotoxic injury model in postnatal brain. Stroke 32, 2394–2402.

76 Wilhelmsson, U., Li, L., Pekna, M., Berthold, C. H., Blom, S., Eliasson, C., Renner, O., Bushong, E., Ellisman, M., Morgan, T. E. and Pekny, M. (2004) Absence of glial fibrillary acidic protein and vimentin prevents hypertrophy of astrocytic processes and improves post-traumatic regeneration. J. Neurosci. 24, 5016–5021.

77 Stefan, C., Gijsbers, R., Stalmans, W. and Bollen, M. (1999) Differential regulation of the expression of nucleotide pyrophosphatases/phosphodiesterases in rat liver. Biochim. Biophys. Acta 1450, 45–52.